Journal of the Korean Physical Society, Vol. 55, No. 4, October 2009, pp. 1357∼1362

Nonlinear Analysis of the Estrous-cycle Time Series in Mice

Tzuyin Wu and Lieh-Jung Chang
Department of Mechanical Engineering, National Taiwan University, Taipei 106, Taiwan

Shu-Yin Wang
Department of Animal Science, Chinese Culture University, Taipei 111, Taiwan

Zhi-Yuan Su*
Department of Information Management, Chia Nan University of Pharmacy & Science, Tainan 717, Taiwan

Yeng-Tseng Wang
National Center for High-performance Computing, Tainan 742, Taiwan

(Received 28 February 2009, in final form 15 July 2009)

A nonlinear time-series analysis method is used to investigate the dynamic behavior of the estrous cycle in female mice. Taking the daily changes in the cell types observed in the vaginal smears of mice as a single-variable time series, we construct a multi-dimensional state space by using an embedding scheme. The Lyapunov exponent and the correlation dimension of the trajectories in the re-constructed state space are analyzed in order to understand the underlying dynamics of the reproductive cycle of the mice. The time-series analysis results are found to be consistent with the physiological description of the reproductive endocrine system. Moreover, the results suggest that the variations in the estrous cycle of mice have a low-dimensional chaotic motion.

PACS numbers: 05.45.Tp, 05.45.-a
Keywords: Estrous cycle, Endocrines, Nonlinear time series, Dynamical system, Chaotic motion
DOI: 10.3938/jkps.55.1357

I. INTRODUCTION

Fluctuating cycles are observed in many common physiological phenomena, including the cardiac rhythm in circulatory systems, calcium oscillation in cell biology, and glycolytic oscillation in metabolic systems. In most cases, this oscillatory behavior does not exhibit a simple periodic nature. In contrast to classical homeostasis principles, which state that physiological systems operate and regulate to maintain relatively stable and equilibrium-like internal states, the oscillation patterns in many biochemical reactions and biological systems are both complex and highly variable. Dynamic systems analysis methods provide a promising approach for understanding such complex oscillatory behavior in both a qualitative and a quantitative manner. In particular, the development of chaos theory has shed much light on the origins of the apparently irregular, periodic oscillations found in a variety of biological and physiological contexts [1–6].

The mathematical modeling of physiological dynamics based on experimental observations is fraught with difficulty. Most experiments are limited to the observation and measurement of just one, or at best two or three, physical quantities. Furthermore, in many cases, the total number of variables governing the behavior of the experimental system is not even clear at the outset. These difficulties can be resolved to a certain extent by utilizing nonlinear time-series analysis methods designed to extract the dynamics from nonlinear systems. Such methods are based on the notion that the information describing the dynamics of a multi-dimensional system is inherently embedded within the time-series record of a single variable. Given the application of a suitable unfolding technique, the trajectories and embedding state space reconstructed from this single-variable data sequence have the same geometric and dynamic properties as those characterizing the state-space dynamics of the original system. The use of a single scalar time series to generate an embedding space and its associated dynamics was originally suggested by Packard *et al.* [7] and was subsequently formulated as the embedology theory by Takens [8] and by Sauer *et al.* [9]. In recent decades, embedology and its associated techniques have been used to analyze experimental data in a variety of fields [10–

*E-mail: zysu@mail.chna.edu.tw; Fax: +886-6-366-0607

17]. In the present study, a time-series analysis technique is applied to examine the estrous cycle in female mice.

The remainder of this paper is organized as follows: Sec. II reviews the hormone function within the biological reproductive endocrine system. Sec. III describes the experimental procedure used to establish a single-variable experimental time series characterizing the phenomenology of the estrous cycle in female mice. Sec. IV analyzes the state-space dynamics of the experimental scalar time series and presents a feasible physiological interpretation of the dynamic-system results. Finally, Sec. V presents some brief conclusions

II. BIOLOGICAL REPRODUCTIVE CYCLE

All female mammals have a reproductive period that begins at puberty and ends with menopause. In non-seasonal breeding animals, most non-pregnant females exhibit a regular physiological change known as the estrous cycle. The length of this cycle is not consistent, but varies with the species, genetics, age, environment and physiological condition of the animal. The estrous cycle of female mice ranges from 3 to 9 days, with an average of 4 to 5 days. The cycle can be divided into proestrus, estrus, metestrus and diestrus stages depending on changes in the ovary, reproductive ducts and endocrine system.

Theoretically, the estrous cycle can be monitored by observing the variations in the plasma hormone profiles. However, the frequent taking of blood samples is not only time consuming but also causes stress to the animal and the stress induces its own effects on the plasma hormone profiles and therefore distorts the experimental observations. Moreover, the volume of blood collected in each sample is too little for most practical analyses. In most female mammals a change in the level of endocrine during the estrus cycle is known to result in a morphological change in the epithelial tissue of the vagina. Therefore, in animals with a short estrous cycle, such as mice, the change in the cell types observed in a vaginal smear provides a useful indication of both the overall length of the estrous cycle and the duration of each stage within it.

III. MATERIAL AND METHODS

Ten female mice (C57BL/6J) were individually caged and raised in an animal room (21 – 25 °C, 12L : 12D). The mice were fed *ad libitum* and were given water freely. After the opening of their vaginas, vaginal smears were collected daily between 13 : 30 and 14 : 30 until the mice reached menopause (12 – 14 months).

In collecting the smears, a drop of clean water was inserted into the vagina and flushed back and forth two or three times by using an eyedropper. The flushed fluid was then dropped on a slide and dried in air. Following the drying process, the smears were examined under a microscope for the existence of leukocytes, nucleated epithelial cells and cornified epithelial cells. The smears were then stained with Leu stain and re-examined under a microscope. The number of each type of cell observed in the stained smears was then recorded for analysis purposes.

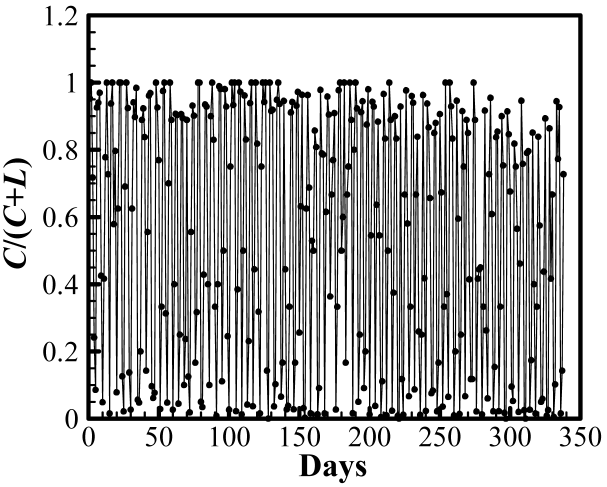

Fig. 1. Daily-recorded values of the cell number ratio.

As described in Sec. II, the change in the cell types observed in the smear closely follows the cyclic change in the reproductive endocrine system. In the present experiments, the daily value of the number of cornified epithelial cells (C) was recorded as a percentage of the total number of cornified epithelial cells and leukocytes (L), *i.e.*, as $C/(C+L)$. This daily value was then taken as a single-variable time series representing the underlying dynamic behavior of the reproductive endocrine system of the female mice.

IV. TIME SERIES ANALYSIS AND DISCUSSION

Figure 1 presents a typical experimental time series $s(n)$ formed by using the daily-recorded values of $C/(C+L)$ for a single mouse. The power spectrum of this fluctuating sequence is given in Fig. 2. The spectrum has a broad-band distribution and has no obvious periodic structure. A broad peak is observed at a frequency of approximately 0.24, which indicates that the average period of the estrous cycle of the mouse is around $4 \sim 5$ days. The scalar time series $s(n)$ presented in Fig. 1 can be used to generate an embedding space of the system of interest via a suitable embedding scheme. The most commonly used embedding technique is the time-delay coordinates method [7], in which the coordinates of the embedding space are constructed from the vector

$$[s(n), s(n+T), s(n+2T), \cdots, s(n+(d-1)T] \qquad (1)$$

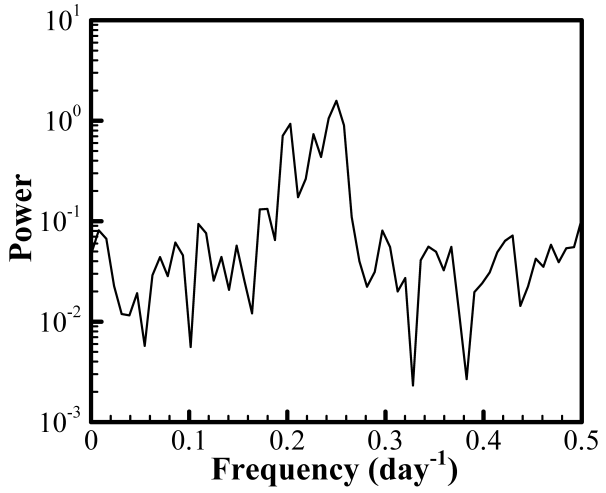

Fig. 2. Typical power spectrum of an experimental time series.

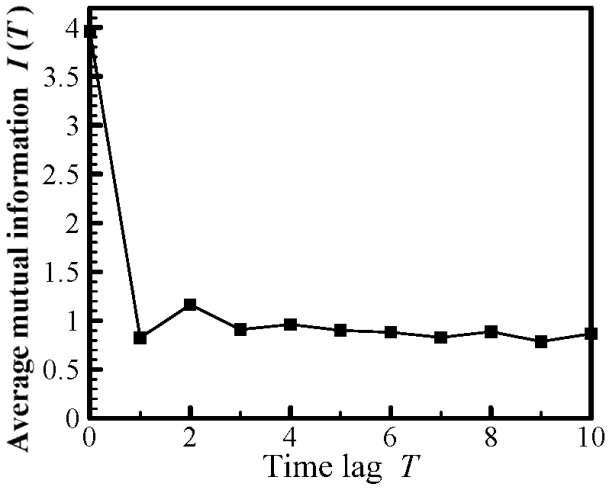

Fig. 3. Variation of the average mutual information $I(T)$ with the time lag T.

where T is the time lag and is generally an integer multiple of the sampling time interval τ_s (1 day in the present experiments); and d is the dimension of the embedding space. Note that in ensuring a proper choice of the time lag T in the present experiments, this study adopted the mutual information concept, $s(n)$ and $s(n+T)$ is given by

$$I(T) = \sum_{\substack{s(n)\\ s(n+T)}} P(s(n), s(n+T)) \log_2 \times \left[\frac{P(s(n), s(n+T))}{P(s(n))P(s(n+T))} \right] \quad (2)$$

where $P(s(n), s(n+T))$ denotes the joint probability distribution of $s(n)$ and $s(n+T)$. The mutual information function $I(T)$ measures the extent to which the data in one time sequence are correlated with those in a second time sequence observed at a time T before. In other words, the information function is a function of the time lag T. A good embedding scheme requires maximum independence between the various coordinates; thus an obvious option for the time lag T is the time at which the mutual information function given in Eq. (5) first exhibits a minimum [18]. Fig. 3 plots the average mutual information as a function of the time lag T for one set of experimental data collected in this study. The first minimum in $I(T)$ can be seen to occur at $T = 1$. A similar result was observed for the experimental data series constructed for each of the ten mice. Thus, the time lag (*i.e.* the interval at which the experimental data were collected) was specified as $T = 1$ day.

A proper embedding space, when interpreted geometrically, is a phase space in which all the tangles and crossings in the trajectories constructed from the time series are virtually 'unfolded' Applying this notion, Kennel *et al.* [19] proposed a geometric scheme for determining the minimum embedding dimension d required to fully unfold a time series. In the proposed scheme, two points that are close within the original d-dimensional space but are far removed when unfolded in the $d+1$-dimensional space are designated as 'false nearest neighbors' (FNNs).

Suppose that a point located in the d-dimensional reconstructed space is described by

$$\bar{y}(n) = [s(n), s(n+T), \cdots s(n+(d-1)T)]. \quad (3)$$

The nearest neighbor to this point, *i.e.* the point which lies at the shortest distance from$\bar{y}(n)$, is given by

$$\bar{y}^{NN}(m) = [s^{NN}(m), s^{NN}(m+T), \cdots s^{NN}(m+(d-1)T)], \quad (4)$$

where m denotes the nearest neighbor point and n is the original point.

However, point $\bar{y}^{NN}(m)$ may be a FNN neighbor arising from a higher-dimension projection. This possibility can be checked by calculating the distance $R_d(n,m)$ between points $\bar{y}(n)$ and $\bar{y}^{NN}(m)$ under dimension d in accordance with

$$R_d^2(n,m) = \sum_{k=1}^{d} [s(n+(k-1)T) - s^{NN}(m+(k-1)T)]^2. \quad (5)$$

When the unfolding dimension is increased to $d+1$, the distance between the two points becomes

$$R_{d+1}^2(n,m) = \sum_{k=1}^{d+1} [s(n+(k-1)T) - s^{NN}(m+(k-1)T)] = R_d^2(n,m) + \left| s(n+dT) - s^{NN}(m+dT) \right|^2. \quad (6)$$

The difference between the two distances can be quantified as follows:

$$\sqrt{\frac{R_{d+1}^2(n,m) - R_d^2(n,m)}{R_d^2(n,m)}}$$

Table 1. Embedding dimensions determined from mice data.

Mouse no.	i	ii	iii	iv	v
Embedding dimension d	6	5	5	5	6
Mouse no.	vi	vii	viii	ix	x
Embedding dimension d	5	6	5	5	6

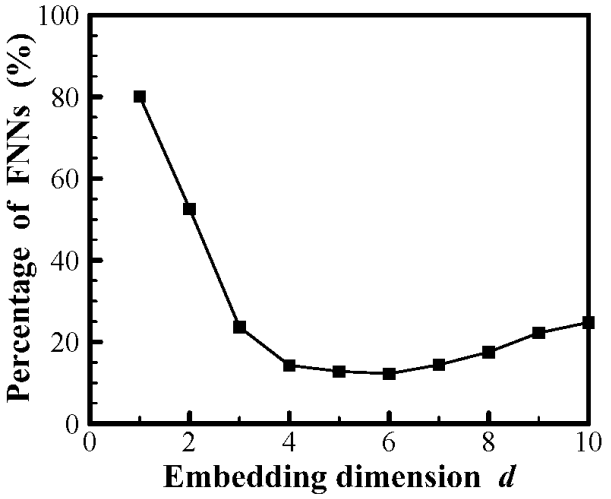

Fig. 4. Variation of the percentage of false nearest neighbors (FNNs) with the embedding dimension.

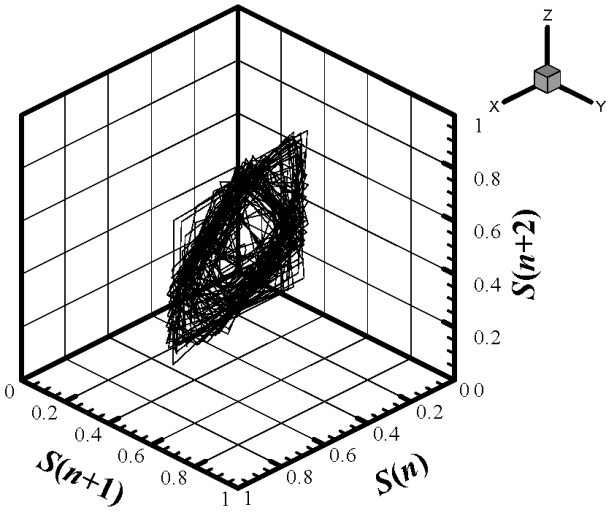

Fig. 5. Projection of trajectories onto three-dimensional state space constructed by using time-delay coordinates.

$$= \frac{\left|s(n+dT) - s^{NN}(m+dT)\right|}{R_d(n,m)}. \qquad (7)$$

If the result exceeds a certain predetermined valueR_{tol}, then $\bar{y}^{NN}(m)$ is a FNN of $\bar{y}(n)$. Note that in most general applications, R_{tol} is assigned a value of 15.

Figure 4 plots the percentage of FNNs as a function of the unfolding dimension for the present experimental time series. It can be seen that the percentage of FNNs decreases initially with increasing unfolding dimension. However, due to the presence of noise, which is generally regarded as a high-dimensional signal in experimental time series, the percentage of FNNs does not decrease to zero, but attains a minimum value and then increases gradually with increasing unfolding dimension. In the present embedding procedure, the optimum embedding dimension is specified as the value of d corresponding to the minimum number of FNNs. Table 1 summarizes the embedding dimensions determined using this method for each of the data sets collected for the ten mice. As shown, the optimum embedding dimension is found to have a value of five or six in every case.

Table 2. Lyapunov exponents calculated from mice data.

Mouse no.	i	ii	iii	iv	v
Lyapunov exponent λ	0.28	0.34	0.26	0.25	0.28
Mouse no.	vi	vii	viii	ix	x
Lyapunov exponent λ	0.32	0.35	0.34	0.34	0.41

Table 3. Correlation dimensions calculated from mice data.

Mouse no.	i	ii	iii	iv	v
Correlation dimension D_c	3.09	3.46	3.64	3.12	3.18
mouse no.	vi	vii	viii	ix	x
Correlation dimension D_c	nil	3.19	4.01	3.31	3.66

Having determined the proper embedding dimension, a reconstructed attractor can be generated from the experimental time series in this d-dimensional embedding space. Since it is impossible to draw any object with more than three dimensions on a simple plane, Fig. 5 shows a 'projection' of the attractor on a three-dimensional space spanned by the time-delay coordinates $(s(n), s(n+1), s(n+2))$. The attractor is observed to have an aperiodic characteristic.

An important invariant property of the reconstructed attractor shown in Fig. 5 is the Lyapunov exponent, which quantifies the divergence rate of nearby trajectories and has a positive value in the event of chaotic motion. Table 2 lists the largest Lyapunov exponent λ for each of the ten data series, as calculated using the method proposed by Wolf *et al.* [20]. Each data series is observed to have a positive Lyapunov exponent; thus the estrus time series in mice appears at first glance to have a chaotic characteristic. However, since noise also features a positive Lyapunov exponent, whether the experimental time series truly represent a chaotic signal or are simply dominated by high-dimensional noise is not conclusive at this point.

Another important invariant quantity characterizing a time series is the correlation dimension of the reconstructed attractor [21]. In general, the value of the cor-

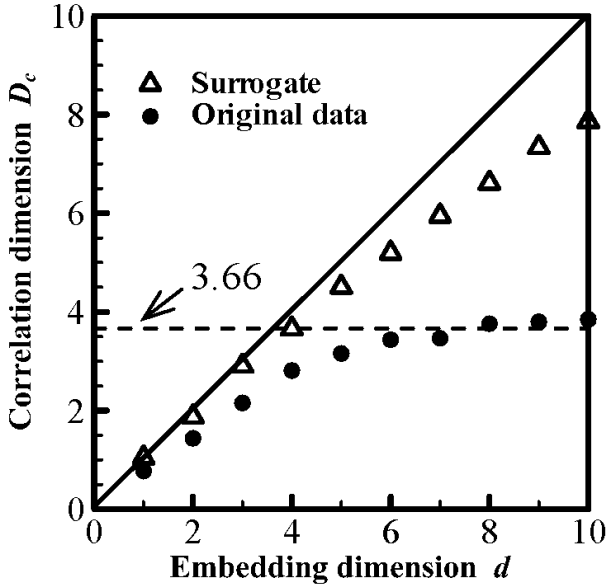

Fig. 6. Variation of the correlation dimension of the attractor with the embedding dimension.

relation dimension varies with the unfolding dimension. Fig. 6 shows the correlation dimensions D_c calculated for one of the current data sets under different embedding dimensions d. D_c is observed to saturate at a value of approximately 3.66 for all $d \geq 6$ (see black symbols). If the time series were dominated by noise, the value of D_c would increase with increasing embedding dimension along the 45 degree line shown in Fig. 6. However, this is clearly not the case in Fig. 6. The well-defined correlation dimension of the reconstructed attractor and the positive Lyapunov exponents listed in Table 2 collectively suggest that the experimental time series are characterized by a low-dimensional chaotic motion. In principle, a surrogate data test is needed to check if low-dimensional chaos exists in estrous cycle. In the method if a linear process is to be specified as a null hypothesis, surrogate data sets that are consistent with the null hypothesis must be generated; then a discriminating statistics for the original and for each surrogate data sets must be computed. If the result computed for the original data is different than the results computed for the surrogate data, then the null hypothesis is rejected and nonlinearity is detected [22] In this paper, we used the unwindowed. Fourier transform (FT) algorithm for generating surrogate data. In Fig. 6, the estimated dimension can be seen to increase almost as rapidly with the embedding dimension for the surrogate data (see white symbol). By comparing the surrogate data to the original data, we can reject the null hypothesis that the data arise from a linear stochastic process and find evidence that the original time series is low-dimensional. Of the ten data series obtained in this study, nine of the series exhibited a characteristic similar to that shown in Fig. 6, except for no. 6 mouse.

Table 3 summarizes the correlation dimension for each of the ten data series. It can be seen that D_c generally has a value between three and four, indicating that the dynamics of the attractor has four active degrees of freedom. Table 1 shows that the present experimental data series have an embedding dimension of five or six. Note that the embedding dimension is determined from a geometric consideration and is therefore not necessarily equal to the number of degrees of freedom of the original system. The present results nevertheless suggest that the reproductive system of mice is described principally by five or six physiological variables.

In biological species, the periodic changes in the female reproductive organs and hormone profiles are regulated by the hypothalamic-pituitary-ovarian (H-P-O) axis of the endocrine system [23]. The function of this H-P-O axis involves several hormones. For example, a gonadotropin-releasing hormone (GnRH) is secreted by the hypothalamus and stimulates secretion of pituitary gonadotropins. Similarly, follicular-stimulating hormones (FSH) and luteinizing hormones (LH) are secreted by the pituitary and stimulate ovarian follicular growth and ovulation, respectively. LH also stimulates the corpus luteum to secrete progesterone and in conjunction with FSH, stimulates estrogen secretion in the follicles. Gonadal steroids (estrogen and progesterone) regulate pituitary gonadotropin secretion via long-loop feedback to the hypothalamus and also exert positive and negative feedback effects at the level of the pituitary [24]. Finally, secreted LH and FSH exert a short-loop feedback inhibition effect on the hypothalamus and may also provide feedback at the level of the pituitary to establish an auto-inhibition effect [25]. In other words, a total of five major participating hormones exist in the stimulation-inhibition control loop, namely GnRH, FSH, LH, estrogen and progesterone. In addition, a recent study found that inhibin, another hormone produced by the ovarian follicular cells, also exerts a feedback inhibition effect on FSH secretion at the level of the pituitary [26]. This might well account for the additional embedding dimension identified in the remaining experimental series.

The correlation dimensions of the reconstructed attractor summarized in Table 3 imply that the local dynamics of the reproductive cycle in mice have around four 'active' degrees of freedom. A possible physiological explanation for this observation is as follows: In this study, the length of the estrus cycle was determined by observing the morphological change in the epithelial cells in vaginal smears. This change is known to be directly affected by the estrogen and the progesterone produced by the ovarian follicular cells [27]. As described above, the secretion profiles of estrogen and progesterone are closely related to the secretion of LH and FSH. Although GnRH can stimulate the secretion of FSH and LH, its effect on estrogen and progesterone is tied up with that of FSH and LH. Furthermore, the inhibitory effects of estrogen and progesterone on GnRH are parallel to those on FSH

and LH. Thus, there is an apparent redundancy in the combined stimulation-inhibition action of GnRH, FSH and LH. Inhibin does not affect estrogen secretion directly, and its inhibitory effect on FSH is parallel to that of estrogen. As a result, the number of major independent factors governing the dynamics of the reproductive cycle is reduced to just four

V. CONCLUSIONS

This study has used a dynamic-systems analysis approach to examine the behavior of the estrous cycle in female mice. A geometric technique has been applied to reconstruct a multi-dimensional state embedding space based upon the single-variable experimental time series obtained from ten mice. The dynamic properties of the experimental time series have been analyzed in terms of the Lyapunov exponent and the correlation dimension. The dynamic properties of the time series have been shown to be consistent with the physiological description of the underlying endocrine function. In addition, the topological properties of the reconstructed attractor suggest that the variability observed in the reproductive cycle of mice is characterized by a low-dimensional ($D_c \leq 4$) chaotic property. The results presented in this study confirm the feasibility of using a nonlinear time-series analysis method to examine the underlying properties of familiar physiological systems.

REFERENCES

[1] L. F. Olsen and H. Degn, Quart. Rev. Biophys. **18**, 165 (1985).

[2] H. Degn, A. V. Holden and L. F. Olsen, *Chaos in Biological Systems* (Plenum Press, New York, 1987).

[3] L. Glass and M. C. Mackey, *From Clocks to Chaos: The Rhythms of Life* (Princeton Univ. Press, Princeton, NJ, 1988).

[4] A. Goldberger, *Biochemical Oscillations and Cellular Rhythms* (Cambridge Univ. Press, Cambridge, 1996).

[5] B. J. West, *Fractal Physiology and Chaos in Medicine* (World Scientific, Singapore, 1990).

[6] M. Barbi and S, Chillemi, *Chaos and Noise in Biology and Medicine* (World Scientific, Singapore, 1998).

[7] N. H. Packard, J. P. Crutchfield, J. D. Farmer and B. S. Shaw, Phys. Rev. Lett. **45**, 12 (1980).

[8] F. Takens, Detecting Strange Attractors in Turbulence, in D. A. Rand and L. S. Young, Dynamical Systems and Turbulence, edited by (Springer-Verlag, Berlin, 1981).

[9] T. Sauer, J. A. Yorke and M. Casdagli, J. Stat. Phys. **65**, 579 (1991).

[10] T. Yazaki, Phys. Rev. E **48**, 1806 (1993).

[11] J. D. Scargle, Astrophys. J. **359**, 469 (1990).

[12] L. I. Aftanas, N. V. Lotova, V. I. Koshkarov, V. P. Makhnev, Y. N. Mordvintsev and S. A. Popov, Int. J. Psychophysiol. **28**, 63 (1998).

[13] J. A. Scheinkman and B. LeBaron, J. Business **62**, 311 (1989).

[14] P. Shang, X. Li and S. Kamae, Chaos, Solitons and Fractals **25**, 121 (2005).

[15] Z. Y. Su, T. Wu, P. H. Yang and Y. T. Wang, Physica A **387**, 2293 (2008).

[16] J. Jeong, Y. Kwak and K. J. Lee, J. Korean Phys. Soc. **46**, 620 (2005).

[17] Y. S. Lim and J. Y. Koo, J. Korean Phys. Soc. **42**, 755 (2003).

[18] A. M. Fraser and H. L. Swinney, Phys. Rev. A **33**, 1134 (1986).

[19] M. B. Kennel, R. Brown and H. D. I. Abarbanel, Phys. Rev. A **45**, 3403 (1992).

[20] A. Wolf, J. B. Swift, H. L. Swinney and J. A. Vastano, Physica D **16** 285 (1985).

[21] P. Grassberger and I. Procaccia, Phys. Rev. Lett. **50**, 346 (1983).

[22] J. Theiler, S. Eubank, A. Longtin, B. Galdrikian and J. D. Farmer, Physica D **58**, 77 (1992).

[23] L. E. Edqvist and G. H. Stabenfeldt, in *Reproduction in Domestic Animals*, edited by G. J. King (Elsevier Science Publishers, New York 1993).

[24] W. E. Stumpf and M. Sar, Fed. Proc. **36**, 1973 (1977).

[25] N. Pattritti-Laborde, A. R. Wolfsen, D. Heber and W. D. Odell, J. Clin. Invest. **64**, 1066 (1979).

[26] L. V. Depaolo, T. A. Bicsak, G. F. Erickson, S. Shimasaki and N. Ling, Proc. Soc. Exp. Biol. Med. **198**, 500 (1991).

[27] R. R. Mehta, J. M. Jenco, L. V. Gaynor and R. T. Chatterton, Jr. Biol. Reprod. **35**, 981 (1986).